Fentanyl inhibits the progression of human gastric carcinoma MGC-803 cells by modulating NF-κB-dependent gene expression *in vivo*

GUODONG HE[1,2*], LI LI[2*], ENJIAN GUAN[2], JING CHEN[2], YI QIN[2] and YUBO XIE[2]

[1]Department of Anesthesiology, The First Affiliated Hospital of Wenzhou Medical University, Wenzhou, Zhejiang 325035; [2]Department of Anesthesiology, The First Affiliated Hospital, Guangxi Medical University, Nanning, Guangxi 530021, P.R. China

Received March 12, 2015; Accepted March 24, 2016

DOI: 10.3892/ol.2016.4619

Abstract. Fentanyl is widely used to treat acute and chronic pain. Previous *in vitro* studies by the present authors demonstrated that fentanyl inhibits the progression of the MGC-803 human gastric carcinoma cell line by affecting apoptosis-related genes, including nuclear factor-kappa B (NF-κB) and phosphatase and tensin homolog. In the present study, the effects of fentanyl on NF-κB-dependent gene expression were investigated *in vivo*. Nude mice were inoculated with an MGC-803 cell suspension, and mice that developed subcutaneous tumors measuring >1.0x1.0 cm were selected for study. Mice were administered intraperitoneal injections of fentanyl (0.05 mg/kg, group F1; 0.1 mg/kg, group F2; 0.2 mg/kg, group F3; and 0.4 mg/kg, group F4) for 14 consecutive days. Non-fentanyl-treated mice (group C) and normal saline-treated mice (group N) served as the control groups. Tumor growth was monitored by calculating the time-shift of the growth curve. Morphological changes were also observed using microscopy. The expression of NF-κB, B-cell lymphoma-2 (Bcl-2), B-cell associated X protein (Bax), vascular endothelial growth factor-A (VEGF-A) and matrix metalloproteinase-9 (MMP-9) in the subcutaneous tumor tissue was also analyzed by reverse transcription-polymerase chain reaction and western blot analysis, and confirmed using immunohistochemistry. The relative tumor volumes of groups F1, F2, F3 and F4 were significantly reduced compared with groups C and N. Furthermore, subcutaneous tumor cells exhibited nuclear swelling, chromatin condensation, reduced chromatin and nuclear fragmentation in the F1, F2, F3 and F4 groups. The number of NF-κB$^+$, Bcl-2$^+$, VEGF-A$^+$ and MMP-9$^+$ subcutaneous tumor cells was reduced, whereas the number of Bax$^+$ cells was increased in the F1, F2, F3 and F4 groups. Additionally, in these groups, tumor expression of NF-κB, Bcl-2, VEGF-A and MMP-9 transcripts and proteins was downregulated, while Bax messenger RNA and protein expression levels were upregulated. The results revealed that fentanyl inhibits the growth of subcutaneous human gastric carcinoma tumors in mice. Therefore, it could be hypothesized that this antineoplastic activity may result from the inhibition of NF-κB activation, suppression of downstream VEGF-A and MMP-9 expression, and normalization of the pro-apoptotic Bax/Bcl-2 ratio.

Correspondence to: Professor Yubo Xie, Department of Anesthesiology, The First Affiliated Hospital, Guangxi Medical University, 6 Shuang-Yong Road, Nanning, Guangxi 530021, P.R. China
E-mail: xieyubo715001@aliyun.com

Abbreviations: NF-κB, nuclear factor-kappa B; Bcl-2, B-cell lymphoma-2; Bax, Bcl-2-associated X protein; VEGF-A, vascular endothelial growth factor-A; MMP-9, matrix metalloproteinase-9; RT-PCR, reverse transcription-polymerase chain reaction

[*]Contributed equally

Key words: fentanyl, gastric carcinoma, NF-κB, Bcl-2, Bax, VEGF-A, MMP-9

Introduction

At present, gastric carcinoma is the fourth most common human neoplasm and the second most common cause of carcinoma-associated mortality worldwide, accounting for 986,600 novel cases and 738,000 mortalities annually (1). The incidence and mortality rates of this disease are higher in China than in other Asian countries (1). The molecular pathogenesis of gastric carcinoma has been investigated extensively with the aim of developing more effective therapeutic strategies for this type of tumor (2). Thus, there is an urgent requirement for the development of strategies to prevent and treat this disease.

Fentanyl, which is the most frequently used analgesic, exhibits minimal cardiovascular effects and does not increase plasma histamine levels (3). Due to its relatively short onset of action and duration of effect, fentanyl is a convenient and widely available drug used in clinical practice (4). As a result of these pharmacological properties, fentanyl is commonly used for the management of severe pain associated with carcinoma (5). A previous study reported that fentanyl inhibited carcinoma cell proliferation and carcinoma progression (6), indicating a

potential antitumor role for this drug (7). However, whether fentanyl affects gastric carcinoma cells remains unclear.

Nuclear factor-kappa B (NF-κB) is a DNA binding protein that regulates cellular activities, including cell cycle, apoptosis, adhesion and angiogenesis, by interacting with its downstream genes (8). A recent study reported that NF-κB-dependent microRNA-425 upregulation promotes gastric carcinoma cell growth by targeting phosphatase and tensin homolog (PTEN) following interleukin-1β induction (9). NF-κB is important in cell development, survival and oncogenesis (10,11). The NF-κB signaling pathway contributes to fentanyl-mediated inhibition of carcinoma cell proliferation (12). However, at present, the association between fentanyl and NF-κB remains unclear.

A previous *in vitro* study by the present authors revealed that fentanyl inhibits the progression of human gastric carcinoma MGC-803 cells via the downregulation of NF-κB and the upregulation of PTEN (7). However, whether fentanyl administration *in vivo* exerts similar effects on the progression of human gastric carcinoma cells remains unclear. Therefore, the present study was conducted to investigate the effects of fentanyl on human gastric carcinoma cells *in vivo* and to explore the possible mechanism that underlies these effects.

Materials and methods

Cell culture. The poorly differentiated MGC-803 human gastric adenocarcinoma cell line was purchased from The Cell Bank of Type Culture Collection of Chinese Academy of Sciences (Shanghai, China). The cells were cultured in Dulbecco's modified Eagle's medium (Invitrogen; Thermo Fisher Scientific, Inc., Waltham, MA, USA) supplemented with 10% heat-inactivated fetal bovine serum (Invitrogen; Thermo Fisher Scientific, Inc.), penicillin (100 U/ml; Gibco; Thermo Fisher Scientific, Inc.) and streptomycin (100 μg/ml; Gibco; Thermo Fisher Scientific, Inc.). The cells were cultured in an incubator with an atmosphere of 5% CO_2 at 37˚C, and the medium was changed every 3 days. A cell suspension was prepared from the cultured cells using a previously described method (13). The viability of the cells in the cell suspension was assessed via trypan blue staining (Sigma-Aldrich, St. Louis, MO, USA).

Animal model and fentanyl administration. Male BALB/C nude mice (4 weeks old; weight, 15-20 g; Vital River Laboratories Co., Ltd., Beijing, China) were used for all experiments. The mice were bred and maintained under standardized housing conditions at a constant room temperature with a 12/12 h light/dark cycle, with access to food and water *ad libitum*. The experimental protocol was approved by the Animal Care and Use Committee of Guangxi Medical University [Nanning, China; approval no. 2016(KY-E-015)]. A murine model of a subcutaneous human gastric carcinoma tumor was established by inoculating the right oxter of each nude mouse with a suspension of cells in logarithmic phase growth. When tumors had grown to 1 cm in diameter, a total of 30 nude mice were randomly divided into the following 6 groups (5 mice per group): Control group (group C), normal saline group (group N), group F1, group F2, group F3 and group F4. Group C received no treatment, group N received an intraperitoneal injection of 1.5 ml/kg saline (daily; GE Healthcare Life Sciences, Logan, UT, USA), and groups F1, F2, F3 and F4 received intraperitoneal injections of 0.05, 0.1, 0.2 and 0.4 mg/kg fentanyl (Yichang Humanwell Pharmaceutical Co., Ltd., Yichang, China), respectively, each day.

Tumor growth curve generation. Following fentanyl administration, the diameter (a) and length (b) of the tumors were measured using a vernier caliper (Saben Int'l Trading (Hong Kong) Co., Ltd., Hong Kong, China) every two days. The tumor volume (TV) was calculated using the following formula: $TV = 1/2 \times (a^2 \times b)$. The relative tumor volume (RTV) was calculated using the following formula: $RTV = TV_n/TV_1 \times 100\%$, where TV_n represents the TV measured at time n, and TV_1 represents the initial TV measurement. The final TV was calculated using the diameter (a) and length (b) measurements that were obtained directly after the tumors were completely resected from the mice. The tumor growth curve was generated using the RTV results.

Morphological observation using microscopy. The nude mice were euthanized via cervical dislocation 16 days after fentanyl administration, and the tumors were completely removed. The resected tumor tissues were paraffin-embedded (Shanghai Huayong Paraffin Co., Ltd., Shanghai, China), fixed in 10% neutral formaldehyde (Tianjin Kermel Chemical Reagent Co., Ltd., Tianjin, China) and dehydrated using a graded ethanol series (Zhejiang Zhongxing Chemical Reagent Co., Ltd, Lanxi, China). A single ultrathin tumor tissue slice (50 nm) was obtained from each mouse using Ultrotome V (LKB, Stockholm, Sweden). The tissue slices were visualized using the Zeiss Axiovert 200 M Inverted Microscope (Zeiss GmbH, Jena, Germany).

Immunohistochemical analysis. Upon fixation with 4% buffered paraformaldehyde (Tianjin Kermel Chemical Reagent Co., Ltd.), tumor tissues were embedded in paraffin and cut into 4-μm sections. For the immunohistochemical analysis of NF-κB, B-cell lymphoma-2 (Bcl-2), B-cell associated X protein (Bax), vascular endothelial growth factor-A (VEGF-A) and matrix metalloproteinase-9 (MMP-9) expression, the sections were deparaffinized using xylene and rehydrated using an ethanol/H_2O gradient, subsequent to heating in an electro-thermostatic drier (DGG-9070A Electro-thermostatic Drier; SenXin Experimental Apparatus Co., Ltd., Shanghai, China) at 60˚C for 20 min, and washed with phosphate-buffered saline (GE Healthcare Life Sciences). Antigen repair was then performed using 50 ml citrate buffer (pH 6.5; Sigma-Aldrich) for 20 min, and the sections were treated with 3% H_2O_2 (Shanghai Lianshi Chemical Reagent Co., Ltd., Shanghai, China) in methanol (Tianjin Siyou Chemical Reagent Co., Ltd., Tianjin, China) for 10 min. The sections were then incubated with rabbit polyclonal anti-NF-κB (dilution, 1:50; catalog no., sc-7151; Santa Cruz Biotechnology, Inc., Dallas, TX, USA), rabbit monoclonal anti-Bcl-2 (dilution, 1:100; catalog no., 2870; Cell Signaling Technology, Inc., Danvers, MA, USA), rabbit monoclonal anti-Bax (dilution, 1:100; catalog no., 14796; Cell Signaling Technology, Inc.), rabbit polyclonal anti-VEGF-A (dilution, 1:100; catalog no., PA1080; Wuhan Boster Biological Technology, Ltd., Wuhan, China) and rabbit polyclonal anti-MMP-9 (dilution, 1:100; catalog no.,

PB9669; Wuhan Boster Biological Technology, Ltd.) primary antibodies. The antibodies were diluted in 1% albumin bovine V (Biosharp Company, Hefei, China). Upon incubation with the donkey anti-rabbit horseradish peroxidase-conjugated secondary antibodies (dilution, 1:10,000; catalog no., sc-2313; Santa Cruz Biotechnology, Inc.), the sections were stained with diaminobenzidine (Beijing CellChip Biotechnology Co., Ltd., Beijing, China).

Reverse transcription-polymerase chain reaction (RT-PCR). Total RNA was extracted from tumor tissues using TRIzol reagent (Tiangen Biotech Co., Ltd., Beijing, China), according to the manufacturer's protocol. RT was performed by incubating total RNA (3 μg), random hexamer primer (1 μl; Invitrogen; Thermo Fisher Scientific, Inc.), 5X reaction buffer (4 μl), RiboLock™ RNase (1 μl), deoxynucleotide triphosphates mix (2 μl) and RevertAid™ M-MuLV reverse transcriptase (1 μl), according to the manufacturer's protocol (Invitrogen; Thermo Fisher Scientific, Inc.). PCR amplification was performed using Taq DNA polymerase (Invitrogen; Thermo Fisher Scientific, Inc.). The expression of the glyceraldehyde 3-phosphate dehydrogenase (GAPDH) gene served as the internal control. The primer sequences were as follows: Forward, 5'-GGGAAGGAACGCTGTCAGAG-3' and reverse, 5'-TAGCCTCAGGGTACTCCATCA-3' for NF-κB; forward, 5'-GACTTCGCCGAGATGTCCAG-3' and reverse, 5'-CATCCCAGCCTCCGTTATCC-3' for Bcl-2; forward, 5'-CCAAGAAGCTGAGCGAGTGT-3' and reverse, 5'-CCGGAGGAAGTCCAATGTC-3' for Bax; forward, 5'-TCACCCCACTAATGGCACC-3' and reverse, 5'-TCCACTTCCCACCAACAGAC-3' for VEGF-A; forward, 5'-ACGACCACGGACAGAGTAGAA-3' and reverse, 5'-GAAGGGACTCAATCAGCAACA-3' for MMP-9; and forward, 5'-ACAGCAACAGGGTGGTGGAC-3' and reverse, 5'-TTTGAGGGTGCAGCGAACTT-3' for GAPDH. The primers were synthesized by Invitrogen (Thermo Fisher Scientific, Inc.). The reaction was performed using a Bio-Rad Thermal Cycler (Bio-Rad Laboratories, Inc., Hercules, CA, USA) at 37˚C for 15 min and 70˚C for 50 min. RT-PCR was performed as follows: Initial denaturation at 94˚C for 4 min; 30 cycles of denaturation at 94˚C for 30 sec, annealing at 55˚C for 30 sec and extension at 72˚C for 45 sec; and final extension at 72˚C for 5 min. Finally, the PCR amplification products were examined using 1.2% agarose gel electrophoresis.

Western blot analysis. Tumor samples (20 mg) were mechanically homogenized in 100-200 μl lysis buffer (Wuhan Boster Biological Technology, Ltd.) and centrifuged (Sorvall ST 16R Centrifuge; Thermo Fisher Scientific, Inc.) at 11,268 x g for 3-5 min at 4˚C. The supernatant was subsequently collected, and the total protein concentration in the supernatant was quantified using a Bradford protein assay (Bio-Rad Laboratories, Inc.). Protein extracts (16 μl/sample) were heated for 10 min at 95˚C and denatured in sodium dodecyl sulfate sample buffer (Invitrogen; Thermo Fisher Scientific, Inc.). The samples and the PageRuler™ Prestained Protein Ladder (Thermo Fisher Scientific, Inc.) were loaded onto a NuPAGE Novex 4-12% Bis-Tris gel (Invitrogen; Thermo Fisher Scientific, Inc.) for electrophoresis, and then transferred to a polyvinylidene difluoride membrane (Bio-Rad Laboratories, Inc.) using the Bio-Rad Mini-Protein Tetra System (Bio-Rad Laboratories, Inc.). The membranes were treated with blocking solution containing 5% non-fat dry milk (Difco™ Skim Milk; Bio-Rad Laboratories, Inc.) in Tris-buffered saline (TBS; Biosharp Company) with 0.1% Tween-20 (Amresco LLC, Cleveland, OH, USA) for 2 h. The membranes were next incubated with the rabbit polyclonal anti-NF-κB (dilution, 1:1,000), rabbit polyclonal Bcl-2 (dilution, 1:1,000), rabbit polyclonal anti-Bax (dilution, 1:1,000), rabbit polyclonal anti-VEGF-A (dilution, 1:500) and rabbit polyclonal anti-MMP-9 (dilution, 1:500) primary antibodies overnight for ~12 h at 4˚C. Following three washes with TBS containing Tween-20, the membranes were incubated with donkey anti-rabbit horseradish peroxidase-conjugated secondary antibodies (dilution, 1:10,000) for 1 h. The immunoreactive bands were visualized using ECL kit (Bio-Rad Laboratories, Inc.). Briefly, the membranes were washed three times with TBS containing Tween-20 for 10 sec each, and incubated with a chemiluminescence reagent for 30-60 sec. The membranes were then exposed to X-ray film in a dark room for 10 sec-15 min. X-ray films were visualized using a gel electrophoresis scanning X-ray imaging analysis system (Gel-Doc XR System; Bio-Rad Laboratories, Inc.), and analyzed using Quantity One analysis software (version 4.6.2; Bio-Rad Laboratories, Inc.). The relative concentrations of NF-κB, Bcl-2, Bax, VEGF-A and MMP-9 were normalized to GAPDH and expressed as a ratio compared with the control.

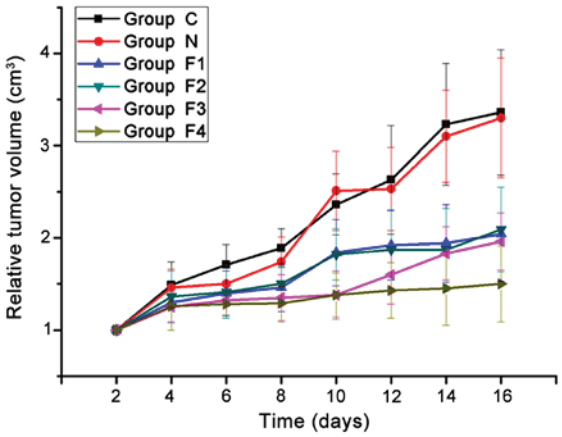

Figure 1. Tumor growth curve. A total of 30 mice were bred and maintained under the same conditions, prior to being divided into 6 groups (n=5 mice/group). Daily intraperitoneal injections of 0.05, 0.1, 0.2 and 0.4 mg/kg fentanyl were administered to groups F1, F2, F3 and F4, respectively, while 1.5 ml/kg saline was administered to group N. Group C received no treatment. The tumor volume was measured every 2 days over the period of 16 days, with 8 time points in total. The differences between the final tumor volumes were assessed for significance. Among the different treatment groups, group F4 showed the maximum effect. The data are expressed as the mean ± standard deviation of 5 mice in each group. Significant differences (P<0.05) were identified as follows: Group C vs. groups F1, F2, F3 and F4; group N vs. groups F1, F2, F3 and F4; and group F4 vs. groups F1, F2 and F3.

Statistical analysis. All data were analyzed using SPSS version 16.0 statistical software (SPSS, Inc., Chicago, IL, USA). Tumor growth data were analyzed using one-way analysis of variance and the Bonferroni method. Western blotting data were statistically analyzed using a two-tailed Student's t-test. All data are expressed as the mean ± standard deviation. P<0.05 was considered to indicate a statistically significant difference.

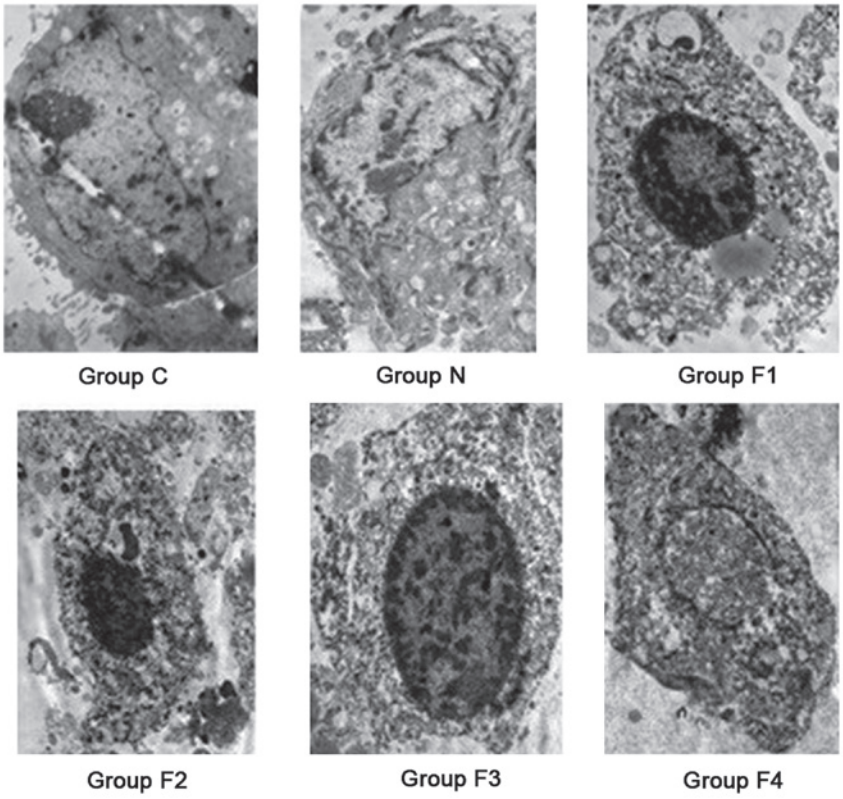

Figure 2. Morphological staining of subcutaneous tumour tissues using 1% uranyl acetate. Nuclear pyknosis, karyolysis and nuclear membrane rupture were observed in groups F1, F2, F3 and F4. Cytoplasmic vacuoles were also observed in groups F1, F2 and F4. There was no significant nuclear abnormality observed in groups C and N. Magnification, x400.

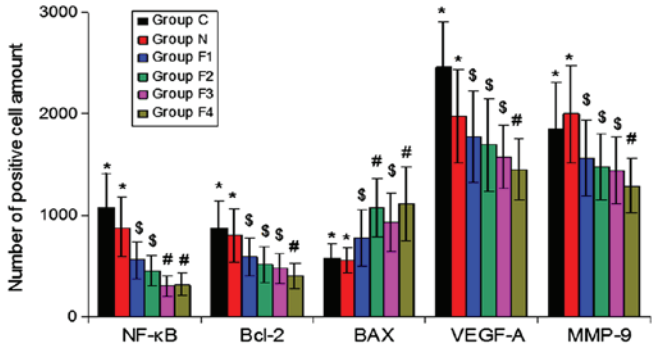

Figure 3. The number of positively stained cells was counted using microscopy. The data are expressed as the mean number of positively stained cells ± standard deviation of 5 mice in each group. Values not sharing a common superscript symbol (*, $ and #) differ significantly at P<0.05. NF-κB, nuclear factor-kappa B; Bcl-2, B-cell lymphoma-2; Bax, Bcl-2 associated X protein; VEGF-A, vascular endothelial growth factor-A; MMP-9, matrix metalloproteinase-9.

Results

Tumor growth curve. Following fentanyl administration, the diameter (a) and length (b) of the tumors were measured every two days. No significant differences were identified in the RTV of groups C or N at any time point (P>0.05). The RTV of groups F1, F2, F3 and F4 were significantly reduced compared with that of groups C and N (P<0.05), however, no statistically significant differences were identified among the fentanyl treatment groups (F1, F2, F3 and F4) (P>0.05) at the first four time points. On day 10 (corresponding to the fifth time point), the RTV of the F3 and F4 groups were significantly reduced compared with the RTV of F1 and F2 groups (P<0.05). On day 16 (eighth time point), the RTV of group F4 was significantly reduced compared with that of groups F1, F2 and F3 (P<0.05) (Fig. 1).

Subcutaneous tumor morphology. Microscopy was used to analyze the morphology of the tumors. In group C, the subcutaneous gastric carcinoma tumor cells exhibited an irregular shape with clear chromatin, increased nucleoli and intact nuclear and cell membranes. Apoptotic morphological changes of varying degrees were observed in groups F1, F2, F3 and F4, where pyknosis, karyolysis, nuclear membrane rupture, cytoplasmic vacuoles and apoptotic bodies were identified. In group N, swollen tumor tissue cells with an irregular shape, large and clear nucleoli and an integrated nuclear membrane were observed (Fig. 2).

Immunohistochemical analysis of NF-κB, Bcl-2, Bax, VEGF-A and MMP-9 protein expression. The percentage of cells exhibiting positive NF-κB, Bcl-2, VEGF-A and MMP-9 expression was reduced in groups F1, F2, F3 and F4 compared with groups C and N. By contrast, Bax expression was increased in groups F1, F2, F3 and F4 compared with groups C and N (P<0.05) (Fig. 3).

NF-κB protein was located in the nucleus, whereas Bcl-2, Bax, VEGF-A and MMP-9 were located in the cytoplasm. In groups C and N, NF-κB, Bcl-2, VEGF-A and MMP-9 were

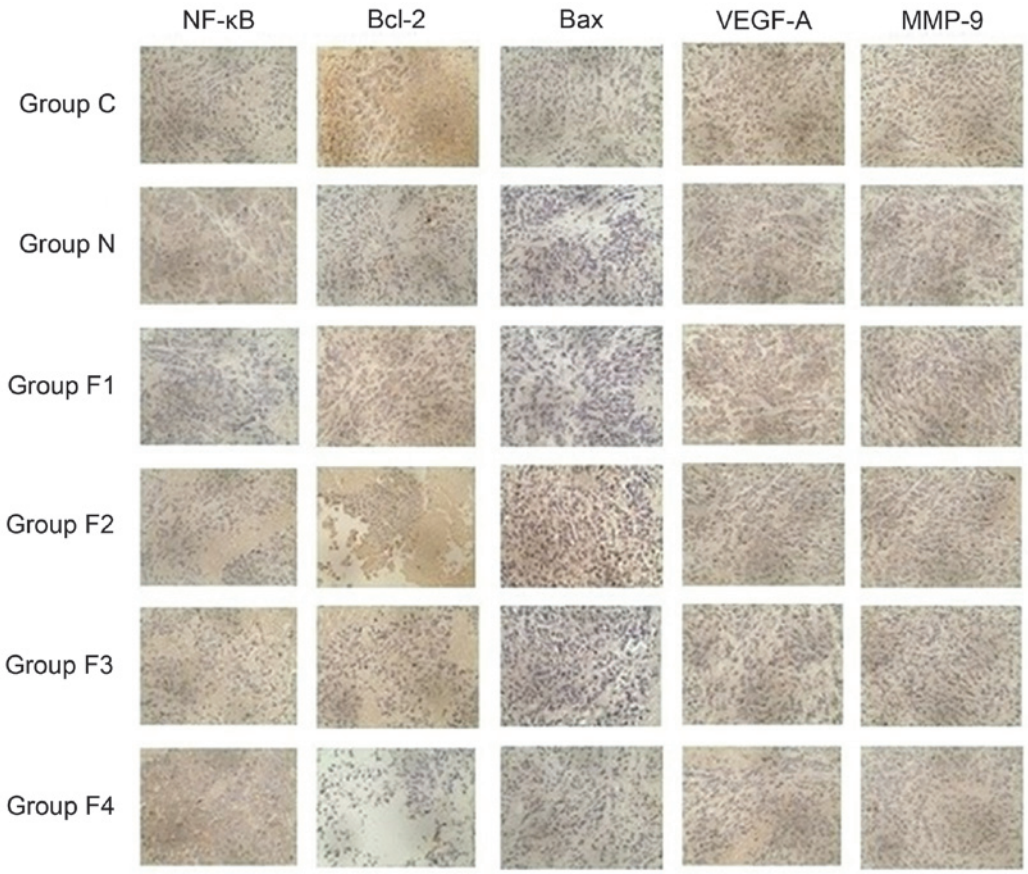

Figure 4. Immunohistochemical staining with 3,3'-diaminobenzidine and hematoxylin indicates positive cells with brown dots (magnification, x40). In groups C and N, intense brown-stained cells indicated overexpression of NF-κB, Bcl-2, VEGF-A and MMP-9. These proteins demonstrated moderate and weak expression in groups F1, F2, F3 and F4. Groups C and N showed a decreased number of brown-stained cells, indicating weak expression of Bax, which was moderately and strongly expressed in groups F1, F2, F3 and F4. NF-κB, nuclear factor-kappa B; Bcl-2, B-cell lymphoma-2; Bax, Bcl-2 associated X protein; VEGF-A, vascular endothelial growth factor-A; MMP-9, matrix metalloproteinase-9.

widely distributed and exhibited strong positive staining throughout the cells, whereas Bax was less widely distributed and exhibited weak staining. By contrast, in groups F1, F2, F3 and F4, NF-κB, Bcl-2, VEGF-A and MMP-9 were less widely distributed and exhibited weak staining, whereas Bax was widely distributed and exhibited strong staining (Fig. 4).

NF-κB, Bcl-2, Bax, VEGF-A and MMP-9 messenger RNA (mRNA) expression. Gel electrophoresis of the RT-PCR products of groups F1, F2, F3 and F4 revealed specific bands corresponding to NF-κB, Bcl-2, VEGF-A and MMP-9 at 321, 259, 321 and 221 bp, respectively. The band intensity indicated that NF-κB, Bcl-2, VEGF-A and MMP-9 mRNA expression levels were increased and BAX mRNA expression levels were decreased in group C and N compared with the fentanyl-treated groups (F1, F2, F3 and F4). In addition, tumor-bearing mice treated with different doses (0.05, 0.1, 0.2 and 0.4) of fentanyl (groups F1, F2, F3 and F4) showed decreased mRNA expression of NF-κB, Bcl-2, VEGF-A and MMP-9, and increased expression of BAX compared with mice in groups C and N, which indicates suppression of tumor growth. Semiquantitative grey ratio analysis of the specific bands and their internal controls was performed using Quantity One software version 4.6.2. The results demonstrated that NF-κB, Bcl-2, VEGF-A and MMP-9 mRNA expression was significantly reduced in groups F1, F2, F3 and F4 compared with groups C and N. In addition, Bax expression was significantly increased in groups F1, F2, F3 and F4 compared with groups C and N ($P<0.05$). No significant differences in NF-κB, Bcl-2, Bax, VEGF-A and MMP-9 mRNA expression were identified between groups C and N (Fig. 5).

NF-κB, Bcl-2, Bax, VEGF-A and MMP-9 protein expression. Analysis of protein expression in groups F1, F2, F3 and F4 revealed specific bands for NF-κB, Bcl-2, VEGF-A and MMP-9 at 65, 26, 27 and 78 kDa, respectively. The western blot analysis showed increased protein expression of NF-κB, Bcl-2, VEGF-A and MMP-9 and decreased expression of BAX protein in groups C and N as compared to fentanyl treated groups (F1, F2, F3 and F4). In addition, treatment of tumor-bearing mice with different doses (0.05, 0.1, 0.2 and 0.4) of fentanyl (F1, F2, F3 and F4) showed decreased protein expression of NF-κB, Bcl-2, VEGF-A and MMP-9, and increased expression of BAX protein compared to mice in groups C and N, which indicates suppression of tumor growth. Semiquantitative analysis demonstrated that NF-κB, Bcl-2, VEGF-A and MMP-9 protein expression in groups F1, F2, F3 and F4 was significantly decreased, while Bax protein expression was significantly increased, compared with groups C and N ($P<0.05$). No significant differences in NF-κB, Bcl-2,

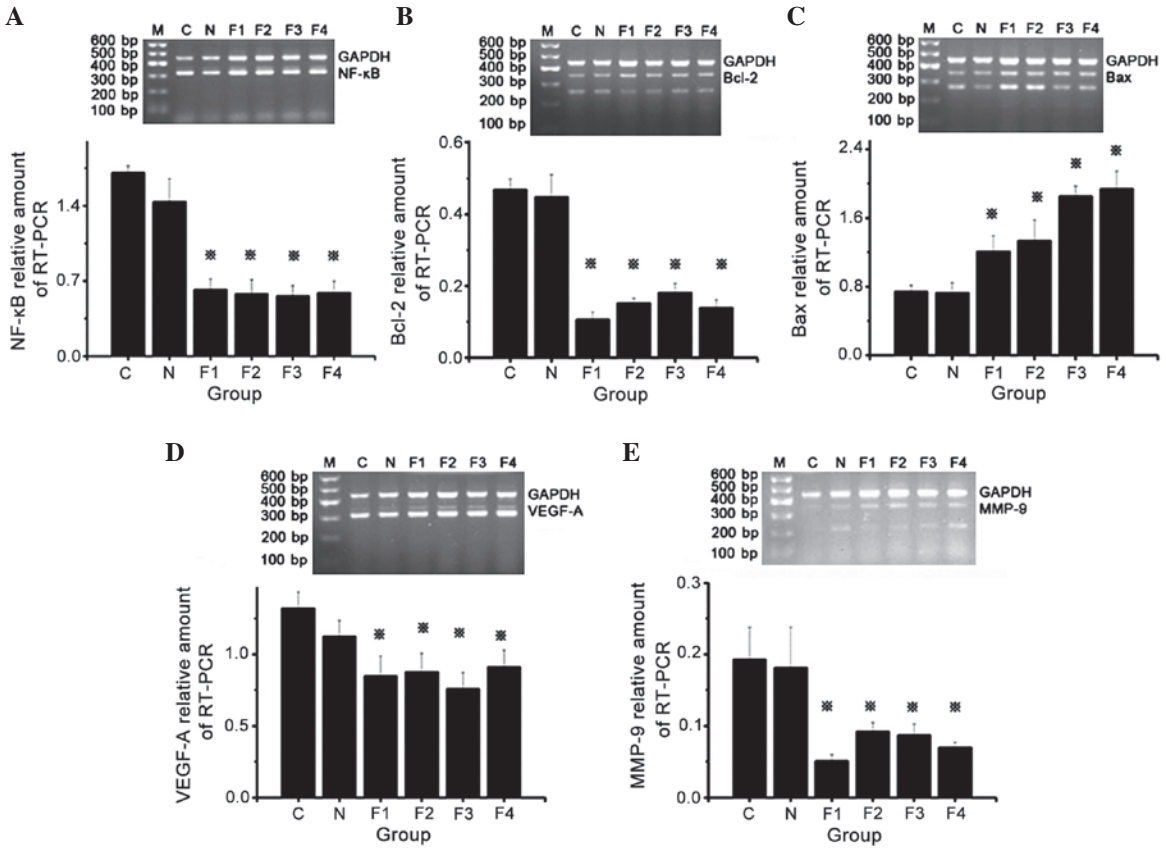

Figure 5. Messenger RNA expression levels of NF-κB, Bcl-2, Bax, VEGF-A and MMP-9 in groups C, N, F1, F2, F3 and F4. (A) Top panel: RT-PCR results of NF-κB and GAPDH expression. Bottom panel: Relative quantification of NF-κB expression. *P<0.05 vs. groups C and N. (B) Top panel: RT-PCR results of Bcl-2 and GAPDH expression. Bottom panel: Relative quantification of Bcl-2 expression. *P<0.05 vs. groups C and N. (C) Top panel: RT-PCR results of Bax and GAPDH expression. Bottom panel: Relative quantification of Bax expression. *P<0.05 vs. groups C and N. (D) Top panel: RT-PCR results of VEGF-A and GAPDH expression. Bottom panel: Relative quantification of VEGF-A expression. *P<0.05 vs. groups C and N. (E) Top panel: RT-PCR results of MMP-9 and GAPDH expression. Bottom panel: Relative quantification of MMP-9 expression. *P<0.05 vs. groups C and N. NF-κB, nuclear factor-kappa B; Bcl-2, B-cell lymphoma-2; Bax, Bcl-2 associated X protein; VEGF-A, vascular endothelial growth factor-A; MMP-9, matrix metalloproteinase-9; RT-PCR, reverse transcription-polymerase chain reaction; GAPDH, glyceraldehyde 3-phosphate dehydrogenase.

Bax, VEGF-A and MMP-9 protein expression were identified between groups C and N (Fig. 6).

Discussion

In a previous *in vitro* study, the present authors demonstrated that fentanyl inhibits the progression of human gastric carcinoma MGC-803 cells via NF-κB downregulation and PTEN upregulation (7). In the present study, a xenograft MGC-803 tumor mouse model was established following the intraperitoneal administration of various doses of fentanyl to nude mice. Subsequently, NF-κB, Bcl-2, Bax, VEGF-A and MMP-9 expression was measured in the subcutaneous tumor tissues. The results revealed that fentanyl inhibits the growth of subcutaneous human gastric carcinoma tumors in nude mice *in vivo*, and promotes gastric carcinoma cell apoptosis by inhibiting the NF-κB signaling pathway and altering the Bcl-2/Bax ratio. Furthermore, the results confirmed that fentanyl inhibits gastric subcutaneous carcinoma invasion and angiogenesis by downregulating VEGF-A and MMP-9 expression.

Fentanyl, which is a potent μ-opioid receptor (MOR) agonist, is considered to be an effective analgesic for cancer pain in terminal cancer patients (14). Lennon *et al* (15) reported that MOR promotes opioid- and growth factor-induced proliferation, migration and epithelial-mesenchymal transition in human lung cancer. A recent study confirmed that fentanyl inhibits tumor growth, increases the expression of sirtuin 1 and decreases he expression of acetyl-p65 in colorectal carcinoma cells via the inhibition of NF-κB activation (16). Thus, the potential antitumor activity of fentanyl must be considered in the management of carcinoma pain. The current study demonstrated that fentanyl-mediated inhibition of tumor cell proliferation and tumor growth is not dose- or time-dependent. In a study by Kampa *et al* (17), opioid alkaloids and casomorphin peptides decreased the proliferation of prostatic carcinoma cell lines in a dose-dependent manner. This discrepancy may be attributed to the different types of carcinoma that were investigated in the two studies. Notably, the present study demonstrated that fentanyl alters cellular morphology, induces cell apoptosis and reduces human gastric carcinoma cell migration.

The transcription factor NF-κB is a DNA binding protein that augments the transcription of various genes that are involved in cell proliferation (18). NF-κB exhibits an important function in cell development (10), survival and oncogenesis (11), which is mediated by the formation of homodimers or heterodimers containing NF-κB/Rel family members, including RelA/p65, RelB, c-Rel, NF-κB1/p50 and NF-κB2/p52 (10,11,19). A variety

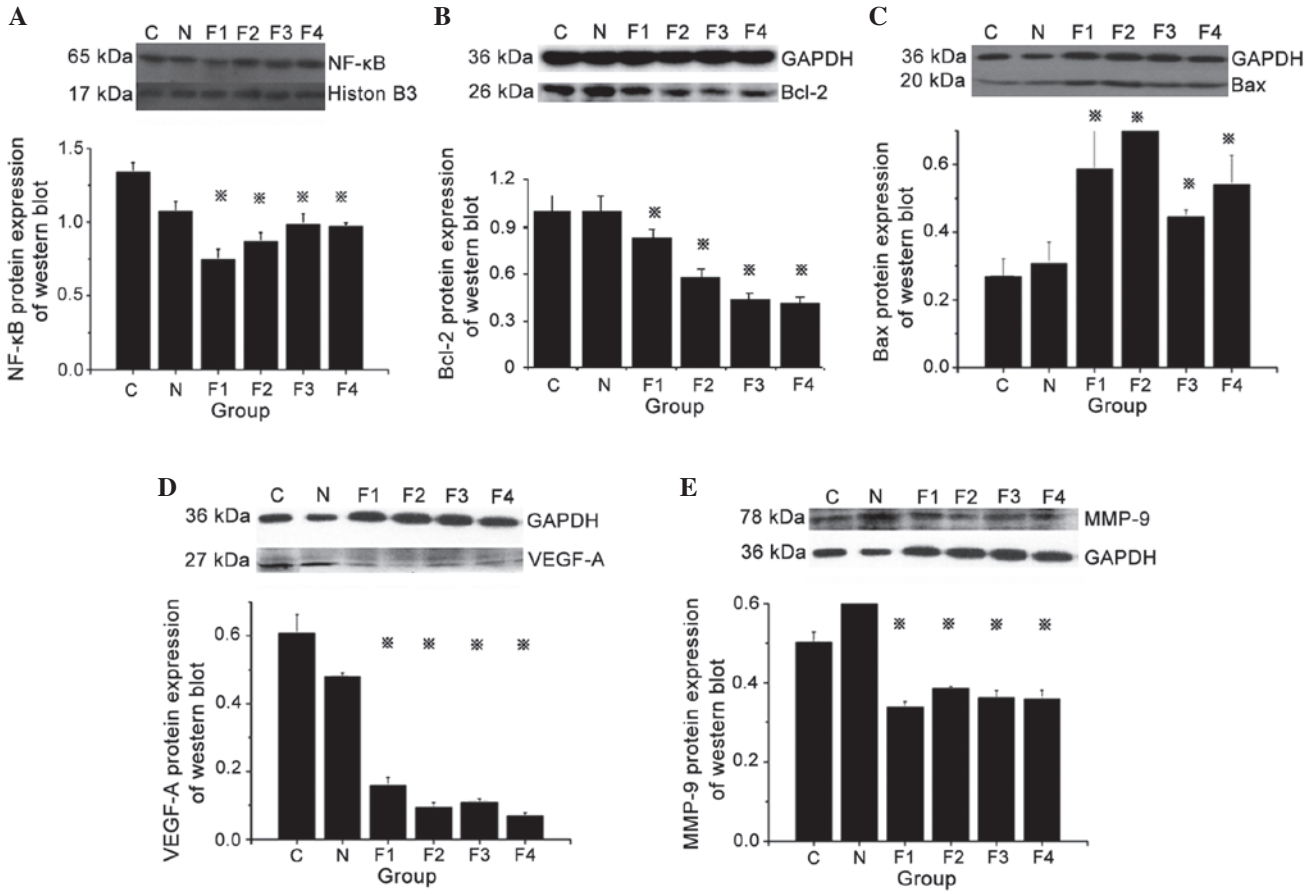

Figure 6. Protein expression levels of NF-κB, Bcl-2, Bax, VEGF-A and MMP-9, as analyzed by western blotting. (A) Top panel: Protein expression of NF-κB and internal control histone. Bottom panel: Relative quantification of NF-κB protein expression. *P<0.05 vs. groups C and N. (B) Top panel: Protein expression of Bcl-2 and internal control GAPDH. Bottom panel: Relative quantification of Bcl-2 protein expression. *P<0.05 vs. groups C and N. (C) Top panel: Protein expression of Bax and internal control GAPDH. Bottom panel: Relative quantification of Bax protein expression. *P<0.05 vs. groups C and N. (D) Top panel: Protein expression of VEGF-A and internal control GAPDH. Bottom panel: Relative quantification of VEGF-A protein expression. *P<0.05 vs. groups C and N. (E) Top panel: Protein expression of MMP-9 and internal control GAPDH. Bottom panel: Relative quantification of MMP-9 protein expression. *P<0.05 vs. groups C and N. NF-κB, nuclear factor-kappa B; Bcl-2, B-cell lymphoma-2; Bax, Bcl-2 associated X protein; VEGF-A, vascular endothelial growth factor-A; MMP-9, matrix metalloproteinase-9; GAPDH, glyceraldehyde 3-phosphate dehydrogenase.

of different stimuli, including cytokines, oxidative stress, apoptosis-inducing stimuli and drugs used in anticancer treatment, are able to activate NF-κB (20,21). Previous studies have demonstrated that morphine directly inhibits NF-κB function via the release of nitric oxide (NO) (22,23). Similarly, in the present study, fentanyl inhibited NF-κB expression in human gastric carcinoma cells. However, whether fentanyl inhibits NF-κB expression and induces antiproliferative and apoptotic effects via the release of NO or via other mechanisms requires further investigation.

Bcl-2, which is a classical anti-apoptotic gene, encodes a 26-kDa transmembrane protein that suppresses apoptosis and subsequently enhances cell survival (24). Bax, which acts as a tumor suppressor, belongs to the Bcl-2 family subgroup of pro-apoptotic genes (25). The Bax protein is a homolog of Bcl-2 and promotes cell death via apoptosis (25). Bax may bind to Bcl-2, forming Bax/Bcl-2 heterodimers, or to itself, forming Bax/Bax homodimers (24). Apoptosis is regulated according to the ratio of these two proteins; specifically, apoptosis is induced by Bax and inhibited by the formation of Bax/Bcl-2 heterodimers (26). Alterations in Bcl-2 and Bax mRNA and protein expression patterns, which typically reflect different prognostic profiles for carcinoma patients, have been identified in human malignancies (27). Bcl-2 is strongly regulated by NF-κB activity (7). NF-κB potentially reduces the Bcl-2/Bax ratio, inducing gastric carcinoma cell apoptosis (28).

The VEGF superfamily critically influences tumor-related angiogenesis (29,30). VEGF promotes neovascularization and migration, and increases vascular permeability (31). VEGF-A is considered the most potent angiogenic factor, and functions by activating the receptor tyrosine kinases VEGF receptor-1 (VEGFR-1) and VEGFR-2 (32). Lee *et al* (33) demonstrated that VEGF suppresses T-lymphocyte infiltration in the tumor microenvironment via the inhibition of NF-κB-induced endothelial activation. The present study revealed that the mRNA and protein expression of NF-κB and VEGF-A decreased in tumor tissues upon fentanyl administration; however, the association between these two proteins remains unclear.

Tumor cells degrade extracellular matrix (ECM) components to invade surrounding tissues (34). This process is tightly controlled by ECM-degrading enzymes, including MMPs (35). MMPs, which are a family of closely-related enzymes that degrade ECM, are involved in tumor invasion and migration, and may be associated with the invasion, lymph node metastasis and survival of gastric carcinoma (36,37). MMP-9 is a zinc-containing enzyme that exhibits potent proteolytic

activity against a wide range of ECM components, including laminin subunit alpha-5 and type IV collagen, which are the major constituents of basement membranes (38). A study performed by Yang *et al* (39) reported positive MMP-9 expression in 60.7% of gastric carcinoma samples. In the present study, positive MMP-9 expression was identified in gastric carcinoma tissues, and it was observed that MMP-9 protein and mRNA expression levels in tumor tissues decreased following fentanyl administration.

In conclusion, fentanyl is recommended as an opioid analgesic in the management of pain in carcinoma patients. The results of present study indicate that fentanyl inhibits the progression of human gastric carcinoma MGC-803 cells by modulating NF-κB-dependent gene expression *in vivo*. Thus, fentanyl is promising for the pain management of cancer patients. However, the mechanism of fentanyl modulation of NF-κB-dependent gene expression requires additional research.

Acknowledgements

The present study was supported by grants from the Natural Science Foundation of China (Beijing, China; grant nos. 81160289 and 81560500) and the Guangxi Science Research and Technology Development Program (Nanning, China; grant no. 1355005-1-6).

References

1. Jemal A, Bray F, Center MM, Ferlay J, Ward E and Forman D: Global cancer statistics. CA Cancer J Clin 61: 69-90, 2011.
2. Tsamandas AC, Kardamakis D, Tsiamalos P, Liava A, Tzelepi V, Vassiliou V, Petsas T, Vagenas K, Zolota V and Scopa CD: The potential role of Bcl-2 expression, apoptosis and cell proliferation (Ki-67 expression) in cases of gastric carcinoma and correlation with classic prognostic factors and patient outcome. Anticancer Res 29: 703-709, 2009.
3. Stanley TH: The fentanyl story. J Pain 15: 1215-1226, 2014.
4. Mystakidou K, Katsouda E, Parpa E, Vlahos L and Tsiatas ML: Oral transmucosal fentanyl citrate: Overview of pharmacological and clinical characteristics. Drug Deliv 13: 269-276, 2006.
5. Seifeldin R and Grossman P: Fentanyl transdermal system and oxycodone hydrochloride. J Manag Care Pharm 9: 457-459, 2003.
6. Huffman DM, Grizzle WE, Bamman MM, Kim JS, Eltoum IA, Elgavish A and Nagy TR: SIRT1 is significantly elevated in mouse and human prostate cancer. Cancer Res 67: 6612-6618, 2007.
7. Qin Y, Li L, Chen J, Tang X, Liao C, Xie Y and Xiao Q: Fentanyl inhibits progression of human gastric cancer MGC-803 cells by NF-kappaB downregulation and PTEN upregulation in vitro. Oncol Res 20: 61-69, 2012.
8. Yang F, Wang H, Jiang Z, Hu A, Chu L, Sun Y and Han J: MicroRNA-19a mediates gastric carcinoma cell proliferation through the activation of nuclear factor-κB. Mol Med Rep 12: 5780-5786, 2015.
9. Ma J, Liu J, Wang Z, Gu X, Fan Y, Zhang W, Xu L, Zhang J and Cai D: NF-kappaB-dependent microRNA-425 upregulation promotes gastric cancer cell growth by targeting PTEN upon IL-1β induction. Mol Cancer 13: 40, 2014.
10. Beg AA, Sha WC, Bronson RT, Ghosh S and Baltimore D: Embryonic lethality and liver degeneration in mice lacking the RelA component of NF-kappa B. Nature 376: 167-170, 1995.
11. Baeuerle PA and Baltimore D: NF-kappa B: Ten years after. Cell 87: 13-20, 1996.
12. Yi J and Luo J: SIRT1 and p53, effect on cancer, senescence and beyond. Biochim Biophys Acta 1804: 1684-1689, 2010.
13. Fabry ME, Kaul DK, Davis L, Gore JC, Brown M and Nagel RL: An animal model for sickle cell vaso-occlusion: A study using NMR and technetium imaging. Prog Clin Biol Res 240: 297-304, 1987.
14. Fusté i Gamisans M and Busquet Duran X: Impact of the commercialization of transdermic fentanyl on the home care of terminal cancer patients. Aten Primaria 29: 316-317, 2002 (In Spanish).
15. Lennon FE, Mirzapoiazova T, Mambetsariev B, Poroyko VA, Salgia R, Moss J and Singleton PA: The Mu opioid receptor promotes opioid and growth factor-induced proliferation, migration and epithelial mesenchymal transition (EMT) in human lung cancer. PLoS One 9: e91577, 2014.
16. Zhang XL, Chen ML and Zhou SL: Fentanyl increases colorectal carcinoma cell apoptosis by inhibition of NF-κB in a Sirt1-dependent manner. Asian Pac J Cancer Prev 15: 10015-10020, 2014.
17. Kampa M, Bakogeorgou E, Hatzoglou A, Damianaki A, Martin PM and Castanas E: Opioid alkaloids and casomorphin peptides decrease the proliferation of prostatic cancer cell lines (LNCaP, PC3 and DU145) through a partial interaction with opioid receptors. Eur J Pharmacol 335: 255-265, 1997.
18. Baldwin AS Jr: The NF-kappa B and I kappa B proteins: New discoveries and insights. Annu Rev Immunol 14: 649-683, 1996.
19. Verma IM, Stevenson JK, Schwarz EM, Van Antwerp D and Miyamoto S: Rel/NF-kappa B/I kappa B family: Intimate tales of association and dissociation. Genes Dev 9: 2723-2735, 1995.
20. Boland MP, Foster SJ and O'Neill LA: Daunorubicin activates NFkappaB and induces kappaB-dependent gene expression in HL-60 promyelocytic and Jurkat T lymphoma cells. J Biol Chem 272: 12952-12960, 1997.
21. Chang CK, Llanes S and Schumer W: Effect of dexamethasone on NF-κB activation, tumor necrosis factor formation, and glucose dyshomeostasis in septic rats. J Surg Res 72: 141-145, 1997.
22. Welters ID, Fimiani C, Bilfinger TV and Stefano GB: NF-kappaB, nitric oxide and opiate signaling. Med Hypotheses 54: 263-268, 2000.
23. Welters ID, Menzebach A, Goumon Y, Cadet P, Menges T, Hughes TK, Hempelmann G and Stefano GB: Morphine inhibits NF-kappaB nuclear binding in human neutrophils and monocytes by a nitric oxide-dependent mechanism. Anesthesiology 92: 1677-1684, 2000.
24. Scopa CD, Vagianos C, Kardamakis D, Kourelis TG, Kalofonos HP and Tsamandas AC: Bcl-2/bax ratio as a predictive marker for therapeutic response to radiotherapy in patients with rectal cancer. Appl Immunohistochem Mol Morphol 9: 329-334, 2001.
25. Oltvai ZN, Milliman CL and Korsmeyer SJ: Bcl-2 heterodimerizes in vivo with a conserved homolog, Bax, that accelerates programmed cell death. Cell 74: 609-619, 1993.
26. Crowson AN, Magro CM, Kadin ME and Stranc M: Differential expression of the bcl-2 oncogene in human basal cell carcinoma. Hum Pathol 27: 355-359, 1996.
27. Jeong SH, Lee HW, Han JH, Kang SY, Choi JH, Jung YM, Choi H, Oh YT, Park KJ, Hwang SC, *et al*: Low expression of Bax predicts poor prognosis in resected non-small cell lung cancer patients with non-squamous histology. Jpn J Clin Oncol 38: 661-669, 2008.
28. Jin Z, Yan W, Jin H, Ge C and Xu Y: Differential effect of psoralidin in enhancing apoptosis of colon cancer cells via nuclear factor-kappaB and B-cell lymphoma-2/B-cell lymphoma-2-associated X protein signaling pathways. Oncol Lett 11: 267-272, 2016.
29. Yancopoulos GD, Davis S, Gale NW, Rudge JS, Wiegand SJ and Holash J: Vascular-specific growth factors and blood vessel formation. Nature 407: 242-248, 2000.
30. Carmeliet P and Jain RK: Angiogenesis in cancer and other diseases. Nature 407: 249-257, 2000.
31. Spyridopoulos I, Luedemann C, Chen D, Kearney M, Chen D, Murohara T, Principe N, Isner JM and Losordo DW: Divergence of angiogenic and vascular permeability signaling by VEGF: Inhibition of protein kinase C suppresses VEGF-induced angiogenesis, but promotes VEGF-induced, NO-dependent vascular permeability. Arterioscler Thromb Vasc Biol 22: 901-906, 2002.
32. Takahashi S: Vascular endothelial growth factor (VEGF), VEGF receptors and their inhibitors for antiangiogenic tumor therapy. Biol Pharm Bull 34: 1785-1788, 2011.
33. Lee SJ, Kim JG, Sohn SK, Chae YS, Moon JH, Kim SN, Bae HI, Chung HY and Yu W: No association of vascular endothelial growth factor-A (VEGF-A) and VEGF-C expression with survival in patients with gastric cancer. Cancer Res Treat 41: 218-223, 2009.
34. Kessenbrock K, Plaks V and Werb Z: Matrix metalloproteinases: Regulators of the tumor microenvironment. Cell 141: 52-67, 2010.

35. Hansson J, Lind L, Hulthe J and Sundström J: Relations of serum MMP-9 and TIMP-1 levels to left ventricular measures and cardiovascular risk factors: A population-based study. Eur J Cardiovasc Prev Rehabil 16: 297-303, 2009.
36. Nissen LJ, Cao R, Hedlund EM, Wang Z, Zhao X, Wetterskog D, Funa K, Bråkenhielm E and Cao Y: Angiogenic factors FGF2 and PDGF-BB synergistically promote murine tumor neovascularization and metastasis. J Clin Invest 117: 2766-2777, 2007.
37. Cao R, Björndahl MA, Religa P, Clasper S, Garvin S, Galter D, Meister B, Ikomi F, Tritsaris K, Dissing S, *et al*: PDGF-BB induces intratumoral lymphangiogenesis and promotes lymphatic metastasis. Cancer Cell 6: 333-345, 2004.
38. Sun WH, Sun YL, Fang RN, Shao Y, Xu HC, Xue QP, Ding GX and Cheng YL: Expression of cyclooxygenase-2 and matrix metalloproteinase-9 in gastric carcinoma and its correlation with angiogenesis. Jpn J Clin Oncol 35: 707-713, 2005.
39. Yang Q, Ye ZY, Zhang JX, Tao HQ, Li SG and Zhao ZS: Expression of matrix metalloproteinase-9 mRNA and vascular endothelial growth factor protein in gastric carcinoma and its relationship to its pathological features and prognosis. Anat Rec (Hoboken) 293: 2012-2019, 2010.